JOURNAL OF SOLID STATE CHEMISTRY 48, 323–332 (1983)

The Comparison of Calculated Transition Probabilities with Luminescence Characteristics of Erbium(III) in Fluoride Glasses and in the Mixed Yttrium–Zirconium Oxide Crystal*

R. REISFELD† AND G. KATZ

Department of Inorganic and Analytical Chemistry,
The Hebrew University of Jerusalem, Jerusalem, Israel 91904

C. JACOBONI AND R. DE PAPE

Laboratoire des Fluorures et Oxyfluorures Ioniques (E.R. CNRS 609),
Université du Maine, F-72017 Le Mans Cedex, France

M. G. DREXHAGE AND R. N. BROWN

Rome Air Development Center, Hanscom AFB, Massachusetts 01731

AND C. K. JØRGENSEN

Département de Chimie minérale, analytique et appliquée,
Université de Genève, CH 1211 Geneva 4, Switzerland

Received December 7, 1982; in revised form February 22, 1983

Fluorozirconate glasses containing 2 mole% ErF_3 were prepared by melting the binary fluorides with ammonium bifluoride under an atmosphere of carbon tetrachloride and argon at 850°C. Absorption spectra of these glasses were obtained and the Judd–Ofelt parameters were calculated. Emission spectra and lifetimes of erbium in fluorozirconate glass, in lead–gallium–zinc fluoride glass, and in yttrium–zirconium oxide crystal were measured and compared with the theoretical calculations. Laser emission lines in these materials are deduced from these measurements. It is suggested that materials doped with erbium may serve as light sources for fiber optic waveguides made from the undoped materials.

1. Introduction

A new family of fluoride glasses was obtained in 1975 by Poulain *et al.* (*1*) in Rennes. They are called fluorozirconate glasses, containing large amounts (above 50 mole%) of ZrF_4 (which can be replaced by HfF_4 or ThF_4) along with lesser amounts of alkaline-earth, rare-earth, or uranium(IV) fluorides (*1–3*). Miranday *et al.* (*29, 30*) prepared another type of new fluoride glasses based on PbF_2 and 3*d*-group fluorides.

Such fluoride glasses (free of BeF_2) exhibit a wide range (0.3 to 7.5 μm) of high

---

* Partially supported by U.S. Air Force Contract AFOSR-F.49620-81-C-012.

† Enrique Berman Professor of Solar Energy.

0022-4596/83 $3.00

transparency, which is exceptionally high in the mid-infrared (2 to 5 μm). They exhibit relatively low refractive indices n in the visible spectral range (between 1.50 and 1.59), and good chemical resistance toward water and weak acids. These glasses have interesting optical properties which make them ideal candidates for producing optical fibers in the mid-ir range (*4, 5*). They represent an improvement over conventional silicate glasses for use in long-distance (above 100 km) repeaterless fiber links for transoceanic or transcontinental communications. One criterion for the high information bandwidth applications is the smallest possible second derivative $d^2n/d\lambda^2$ of the refractive index n; this quantity actually vanishes for a wavelength λ_0 somewhere before the onset of the ir edge (*6*).

The superior characteristics of fluoride glasses for ir fiber optic applications also provide an ideal medium or host enabling the glass to be integrated into a system acting as a laser light source as well as the actual waveguide material. The spectroscopic and fluorescent properties of Nd^{3+} containing fluorozirconate glasses have been reported by Weber in work with the Lucas–M. Poulain (*7*) group at Rennes. To the best of our knowledge, the present work represents the first spectroscopic characterization of erbium in fluorozirconate glass.

In the calculation of radiative transition probabilities, branching ratios, and peak cross section for stimulated emission of Er(III), in the fluoride glasses discussed in this paper, we are using the Judd–Ofelt theory which is described in detail for the present case in (*8*) and (*9*).

The matrix elements $U^{(2)}$, $U^{(4)}$, and $U^{(6)}$ for Er^{3+} in the present glasses as obtained from the measured electronic levels do not differ from those in other fluoride glasses. On the other hand, the three intensity parameters $\Omega_t (t = 2, 4, 6)$ differ quite significantly, as will be seen in the results. The radiative transition probabilities A are connected to the peak cross section for stimulated emission σ_p, which is essential in predicting laser performance, by

$$\sigma_p = \frac{\lambda^4 A}{8\pi c n^2 \Delta\lambda}$$

in units of centimeters squared.

Whereas the Judd–Ofelt theory was originally applied to absorption spectra (*8, 10–14*), the same parameters can be used, with a marginally larger uncertainty, for radiative transition probabilities (*8, 9, 12, 14, 15*) in fluorescence spectra. This approach becomes particularly fruitful in low-phonon fluoride and sulfide glasses where several excited J levels are observed to emit narrow lines, even at room temperature. For the description of the competing nonradiative processes (preventing detectable luminescence in most other materials), other theoretical tools are needed (*12, 16*). On the other hand, the branching ratios from a given luminescent level to a variety of lower J levels (including the ground state) can be compared directly with the Judd–Ofelt theory (*8, 9, 12*), including recent work (*17, 18*) on $4f^6$ europium(III).

2. Experimental

The fluorozirconate glasses with batch compositions of (mole%) $57ZrF_4 : 34BaF_2 : 3LaF_3 : 4AlF_3 : 2MF_3$ (where M represents Er, but other lanthanides can also be incorporated) were prepared in the Hanscom Laboratory using commercially available binary fluorides of 99% or better purity. Batches 10 to 50 g were mixed with 15 g ammonium bifluoride ($NH_4^+FHF^-$) as a precaution against a trace oxide contamination. The glasses were melted over periods of about 5 hr in vitreous carbon crucibles in a resistance-heated furnace under an atmosphere of carbon tetrachloride and argon. This gas mixture was obtained by bubbling argon through CCl_4 at room temperature at such a rate that 10 g CCl_4 were evaporated during the course of a melt cycle. The purpose of this treatment was to reduce oxide and hydroxyl levels in the glass (*19*). Maximum temperatures of ~850°C were required to ensure complete melting; at this point the glasses were cast into cylindrical boron nitride molds, annealed overnight near the glass transition (~300°C), and cooled slowly to ambient temperature. The resulting cylinders, about 1.0 × 1.5 cm diameter, were then ground and polished on opposite faces using standard optical finishing techniques.

A sample $57ZrF_4:36BaF_2:3LaF_3:4AlF_3$ (not doped with other lanthanides) exhibited a glass transition temperature of T_g = 310°C, and a crystallization temperature of T_x = 390°C. It had the density 4.61 g/cm^3 and a refractive index $n_D = 1.52735$. The thermal expansion coefficient between 25 and 200°C was $187.10^{-7}(°C)^{-1}$.

The preparation of $46PbF_2:30GaF_3:22ZnF_2:2LaF_3$ (further doped with 2 wt% ErF_3) was described in this Journal (*8*).

The absorption spectra of the fluoride glasses were measured on a Cary-14 spectrophotometer using undoped (but otherwise identical) glasses as blanks. The excitation and emission spectra were measured with an apparatus built in Jerusalem, and constructed from an Oriel xenon dc 150W source using the excitation monochromator Oriel 7240 with a resolution of 6 nm/mm blazed at 280 nm, further on a Spex 1704 analyzing monochromator blazed at 700 nm, and finally a RCA 7102 Peltier-cooled photomultiplier coupled with a PAR 189 selective amplifier and a PAR 128 lock-in amplifier. The optical system is designed to optimize input to the detector. Since the S-1-type photomultiplier tube (PMT) has an almost vanishing sensitivity above 1100 nm, the emission spectra above this wavelength were measured with a lead sulfide photoconducting crystal cooled by the Peltier effect to −45°C. The PbS output was coupled through PAR lock-in and selective amplifiers to a recorder synchronized with the grating drive mechanism of one of the Oriel 7240 monochromators blazed at 1 μm, thus providing a plot of relative fluorescence as a function of wavelength; another Oriel monochromator was used for varying the exciting photon energies.

The decay curves of luminescence were obtained by exciting the doped glasses with a Molectron DL-200 tunable dye laser equipped with a scan control unit and pumped by a Molectron UV-400 pulsed N_2 laser. The dye used for excitation at 515 nm

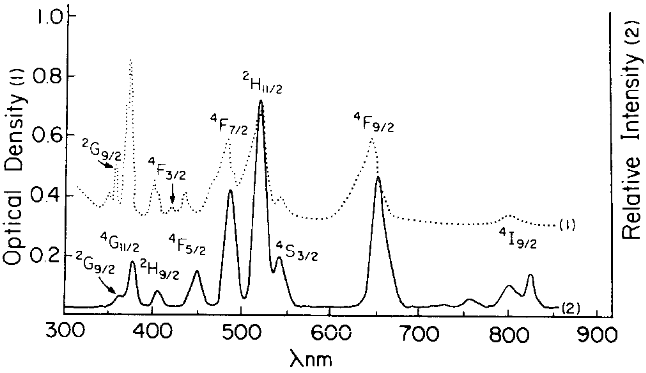

FIG. 1. Comparison of absorption and excitation spectra of erbium(III) in fluoride glass containing lead, zinc, and gallium, at 300 K (=27°C). 2 wt% $ErF_3:46PbF_2 \cdot 22ZnF_2 \cdot 30GaF_3 \cdot 2LaF_3$ (mole%) glass. (1) Absorption. (2) Excitation: λ_{emis} = 975 nm, $^4I_{11/2} \rightarrow {}^4I_{15/2}$. *t* 2.2 mm.

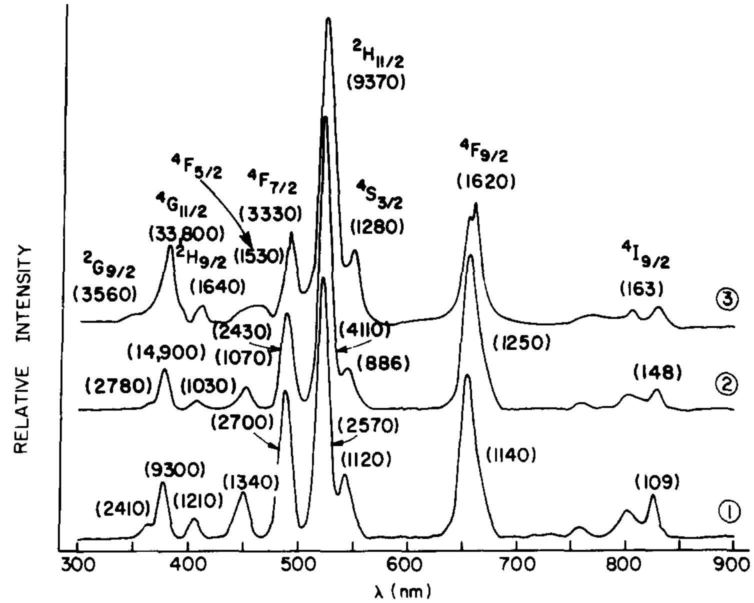

FIG. 2. Comparison of excitation spectra of erbium(III) in two fluoride glasses and in the cubic zirconia–yttria crystal, at 300 K. (1) 2.00 wt% $ErF_3 \cdot 46PbF_2 \cdot 22ZnF_2 \cdot 30GaF_3 \cdot 2LaF_3$ (mole%) glass. (2) 2.66 wt% $ErF_3 \cdot 57ZrF_4 \cdot 34BaF_2 \cdot 3LaF_3 \cdot 4AlF_3$ (mole%) glass. (3) 0.55 wt% $Er_2O_3 \cdot 67ZrO_2 \cdot 33Y_2O_3$ (mole%) stabilized cubic crystal. $\lambda_{emis} = 975$ nm, ${}^4I_{11/2} \rightarrow {}^4I_{15/2}$; PMT S-1 detector.

was C-485, and at 655 nm was R6G. The signal, which was normalized to the intensity of the laser pulse, was fed into a PAR 162/164 boxcar averager, triggered by the laser, and recorded on an $X-Y$ recorder. It was possible to detect the decay after only 2.10^{-8} sec.

3. Results

In Fig. 1, the absorption spectrum of the fluoride glass prepared in Le Mans (*8*) is compared with the excitation spectrum corresponding to the emission at 975 nm from ${}^4I_{11/2}$ to the ground state ${}^4I_{15/2}$. As is frequently the case for lanthanides, a close correspondence is noted with the excitation spectrum (if anything, the latter bands are narrower). The 10 J levels between ${}^4I_{9/2}$ and ${}^2G_{9/2}$ are well established (*12, 13*) as indicated in Fig. 1. There is only one further absorption band in the infrared, corresponding to the first excited level ${}^4I_{13/2}$. However, as we shall see below in Table III, there are good reasons to believe that the cascading down to ${}^4I_{11/2}$ is not systematic from each of the higher J levels, and that the Er(III) state at this point is quite different from that of ${}^5D_0$ in Eu(III) (*12, 17*) and from that of ${}^5D_4$ in Tb(III).

In Fig. 2, the excitation spectrum of Fig. 1 is compared with the corresponding excitation spectra of the fluorozirconate glass and of the yttria–zirconia crystal. Again, the most striking difference from the absorption spectra is that ${}^4G_{11/2}$ seems disproportionally weak in the excitation spectrum, presumably due to efficient nonradiative transitions to slightly lower levels.

Table I treats the observed and calculated oscillator strengths f (called P by many authors) of absorption bands of Er(III) in the fluorozirconate glass, for which the wavenumber and the energy of the transitions are given. Comparable

TABLE I

COMPARISON OF EXPERIMENTAL AND CALCULATED OSCILLATOR STRENGTHS OF ERBIUM(III) IN FLUOROZIRCONATE GLASS

Transition	Wave number (cm^{-1})	$f \times 10^6$ (observed)	$f \times 10^6$ (calculated)
$^4I_{15/2} \rightarrow {}^4I_{13/2}$	6540	1.735	1.63
$^4I_{11/2}$	10260	0.542	0.51
$^4I_{9/2}$	12580	0.287	0.38
$^4F_{9/2}$	15380	1.857	2.13
$^4S_{3/2}$	18520	0.462	0.42
$^2H_{11/2}$	19270	4.880	5.39
$^4F_{7/2}$	20580	1.514	1.86
$^4F_{5/2}$	22320	0.476	0.52
$^4F_{3/2}$	22730	0.194	0.31
$^2H_{9/2}$	24690	0.510	0.68
$^4G_{11/2}$	26450	10.589	10.35
$^2G_{9/2}$	27550	1.987	1.49
$^2K_{15/2}$	28170	0.545	0.48

results for the glass (to which 2 wt% ErF_3 had been added) with molar composition $46PbF_2 : 22ZnF_2 : 30GaF_3 : 2LaF_3$ were presented in Table II of Ref. (*8*), and for the fluorite-type mixed oxide in Table II of Ref. (*9*). In each case, the column "calculated" (and not "adjusted") corresponds to the last column of Table I. It is noted that the Judd–Ofelt predictions are remarkably accurate, the deviation $|f_{obs} - f_{calc}|/f_{obs}$ being 19% on the average, and the absolute value of the deviation $|f_{obs} - f_{calc}|$ being $0.2 \cdot 10^{-6}$ on the average. These values are similar to those of the other fluoride glass (*8*), namely, 18% and $0.15 \cdot 10^{-6}$. However, the latter value is smaller, simply because the two hypersensitive transitions to $^2H_{11/2}$ and $^4G_{11/2}$ are twice as strong in the fluorozirconate glass. It is observed from Table I that there is a mild tendency for the deviations from the Judd–Ofelt theory to grow stronger with increasing wavenumbers.

Table II lists the Ω_t parameters (in the following given in the convenient unit 10^{-20} cm^2) for various Er(III) systems, arranged according to increasing Ω_2 (i.e., according to their increasing propensity toward pseudo-quadrupolar hypersensitive transitions). Though quite extreme values were found by Carnall (*13*) for trivalent lanthanides in molten mixtures of lithium and potassium nitrates, there is little doubt that gaseous $ErCl_3$, $ErBr_3$, and vapors of ternary halides (*22*) such as $Er(Cl_2AlCl_2)_3$ and related species have even larger Ω_2 values. Judd (*23*) has reverted to the suggestion, made in 1964, that high Ω_2 values occur in molecules and in condensed matter in cases wherever it is a dubious approximation to introduce a homogeneous dielectric constant, and evidence is rapidly accumulating that large Ω_2 are indicative of a kind of chemical polarizability (*24*, *25*). It may also be noted in Table II that Ω_6 is largest for solutions, somewhat smaller for glasses, and smallest for the cubic crystals (though the local site for Er(III) is by no means cubic). It is conceivable that Ω_6 decreases with increasing viscosity of the solvent, and is smallest in rigid crystals. In this sense, Ω_6 may represent the average dispersion away from the symmetric nuclear positions on an instantaneous picture. However, this cannot be a simple question of low symmetry, since three quarters of the Y(III) sites in Y_2O_3 belong to the point group C_2.

TABLE II

INTENSITY PARAMETERS Ω_t (IN THE UNIT 10^{-20} cm^2) OF ERBIUM(III) IN SEVEN TYPICAL ENVIRONMENTS

	Ω_2	Ω_4	Ω_6
2 wt% ErF_3 in $46PbF_2 : 22ZnF_2 : 30GaF_3 : 2LaF_3$ glass (*8*)	1.54	1.13	1.19
Er(III) aqua ion, solution (*13*)	1.59	1.95	1.90
Er(III) in fluorite $Y_{0.5}Zr_{0.5}O_{1.75}$ crystal (*9*)	2.92	0.78	0.57
$2ErF_3 : 57ZrF_4 : 34BaF_2 : 3LaF_3 : 4AlF_3$ glass	3.26	1.85	1.14
Er(III) in cubic *C*-type Y_2O_3 crystal (*21*)	4.59	1.21	0.48
$ErW_{10}O_{35}^{-7}$, solution (*11*)	6.7	2.3	1.4
Er(III) in molten $LiNO_3 + KNO_3$ (*28*)	15.8	1.8	1.4

Once the three material parameters Ω_t are sufficiently established from, say, the first 12 absorption bands of a given Er(III) system, it becomes instructive (*14, 15, 17, 18*) to compare them with the transition probabilities $A(J_1, J_2)$ between the levels J_1 and J_2. In such a case, the branching ratio β_{12} is given by $A(J_1, J_2)/\Sigma A$ where ΣA is the sum of all transition probabilities going from J_1 to all lower J_2 levels. However, one has also to take multiphonon relaxation rates W into account (*12, 16*) which are related to the measured (exponential) lifetimes τ_{obs} by

$$W = (1/\tau_{\text{obs}}) - \Sigma A \quad (1)$$

and the quantum yield of luminescence is

$$\eta = \Sigma A/(W + \Sigma A). \quad (2)$$

In the great majority of all J_1 levels of lanthanides, W is much larger than ΣA, and luminescence is almost impossible to detect.

Table III gives the calculated oscillator strengths f and radiative parameters A_{12} and β_{12} for all transitions involving the seven lowest J levels in the fluorozirconate and in the lead–gallium–zinc fluoride glass. At the moment, it is not feasible to evaluate experimentally all the many transitions cascading down in such a 12-level system. The tabulations for the remaining transitions are available as a NAPS document.[1]

An additional complication is that two excited J levels may be situated within a distance of a few units of kT at the prevailing temperature. In cases (*26*) such as Bi(III), the concomitant thermal equilibrium (corresponding to a Boltzmann distribution relative to the lower excited state functioning as ground state) has a strong influence on the luminescence, even at low T. In Er(III), the example of major practical importance is $^2H_{11/2}$ situated only 640 cm^{-1} above $^4S_{3/2}$. In Ref. (*8*), Eq. (12) describes the consequences of this thermalization on the effective radiation transition probability in the lead–zinc–gallium fluoride glass. The same treatment using the parameters $\Sigma A(^2H_{11/2}) = 4410$ sec^{-1} and $\Sigma A(^4S_{3/2}) = 1351$ sec^{-1} with the observed distance 750 cm^{-1} in the zirconium–barium fluoride glass (at $kT = 209$ cm^{-1}) yields $A_{\text{eff}} = 1586$ sec^{-1}.

Figure 3 gives the emission spectra of Er(III) between 500 and 1050 nm in the three samples excited into $^4F_{7/2}$ at 490 nm. All the numbers given in parentheses on Fig. 3 are in units of sec^{-1}. Parentheses without right-hand subscripts represent A for the transition shown. Total radiative transition probabilities ΣA for the excited level considered are marked T, and the A_{eff} values evaluated for the thermalization of $^2H_{11/2}$ and $^4S_{3/2}$ are provided with the subscripts Th. The nonradiative transition probabilities W evaluated according to Eq. (1) are indicated by the subscript NR.

Figure 4 shows the emission spectra in the near infrared region between 900 and 1700 nm. The five numbers given in parentheses represent A(sec^{-1}) for the two transitions. The main reason for failure to detect the $^4I_{11/2} \rightarrow {}^4I_{15/2}$ emission in the yttria–zirconia crystal seems to be the much more effective nonradiative relaxation across the energy gap 3780 cm^{-1} between $^4I_{11/2}$ and $^4I_{13/2}$ in this mixed oxide (*9*) as compared to the two fluoride glasses.

Table IV compares the observed lifetimes τ (in the unit 10^{-6} sec) at 28°C of the three materials, as measured for three wavelengths (corresponding to two transi-

---

[1] See NAPS document No. 04095 for 3 pages of supplementary material. Order from ASIS/NAPS, Microfiche Publications, P.O. Box 3513, Grand Central Station, New York, NY 10163. Remit in advance $4.00 for microfiche copy or for photocopy, $7.75 up to 20 pages plus $.30 for each additional page. All orders must be prepaid. Institutions and organizations may order by purchase order. However, there is a billing and handling charge for this service of $15. Foreign orders add $4.50 for postage and handling, for the first 20 pages, and $1.00 for additional 10 pages of material. Remit $1.50 for postage of any microfiche orders.

TABLE III

RADIATIVE CHARACTERISTICS OF TRANSITIONS BETWEEN THE LOWEST SEVEN *J* LEVELS OF Er(III) IN FLUOROZIRCONATE AND PbGaZn FLUORIDE GLASSES

	$2ErF_3:57ZrF_4:34BaF_2:3LaF_3:4AlF_3$				2 wt% $ErF_3:46PbF_2:30GaF_3:22ZnF_2:2LaF_3$			
	λ(nm)	$f \cdot 10^6$	$A(\sec^{-1})$	β_{12}	λ(nm)	$f \cdot 10^6$	$A(\sec^{-1})$	β_{12}
$^2H_{11/2} \rightarrow {}^4S_{3/2}$	13351	0.003	0.029	0.0000	15601	0.019	0.014	0.0000
$^4F_{9/2}$	2575	0.559	13.0	0.0029	2625	0.285	7.15	0.0025
$^4I_{9/2}$	1495	0.921	63.6	0.0144	1491	0.656	51.1	0.0181
$^4I_{11/2}$	1110	0.520	65.2	0.0148	1122	0.364	50.1	0.0177
$^4I_{13/2}$	786	0.632	158	0.0358	790	0.552	153	0.0542
$^4I_{15/2}$	519	7.18	4110	0.9321	521	4.03	2570	0.9075
$^4S_{3/2} \rightarrow {}^4F_{9/2}$	3191	0.034	0.514	0.0004	3157	0.038	0.662	0.0004
$^4I_{9/2}$	1684	0.979	53.3	0.0394	1648	0.958	61.0	0.0359
$^4I_{11/2}$	1210	0.266	28.0	0.0207	1208	0.287	34.0	0.0200
$^4I_{13/2}$	835	1.73	383	0.2835	832	1.94	486	0.2861
$^4I_{15/2}$	540	1.68	886	0.6559	539	1.88	1120	0.6577
$^4F_{9/2} \rightarrow {}^4I_{9/2}$	3564	0.388	4.71	0.0034	3448	0.326	4.74	0.0038
$^4I_{11/2}$	1950	1.46	59.1	0.0431	1958	1.50	67.6	0.0536
$^4I_{13/2}$	1131	0.511	61.6	0.0450	1129	0.376	51.0	0.0404
$^4I_{15/2}$	650	3.41	1250	0.9085	650	2.78	1140	0.9022
$^4I_{9/2} \rightarrow {}^4I_{11/2}$	4307	0.240	1.99	0.0104	4531	0.022	0.183	0.0012
$^4I_{13/2}$	1656	0.733	41.2	0.2159	1679	0.800	49.1	0.3113
$^4I_{15/2}$	795	0.605	148	0.7737	801	0.402	109	0.6875
$^4I_{11/2} \rightarrow {}^4I_{13/2}$	2691	1.14	24.4	0.1801	2667	1.17	28.5	0.1836
$^4I_{15/2}$	975	0.684	111	0.8199	973	0.693	127	0.8164
$^4I_{13/2} \rightarrow {}^4I_{15/2}$	1529	1.86	122	1.0000	1532	1.94	143	1.0000

TABLE IV

OBSERVED LIFETIMES AND CALCULATED TRANSITION PROBABILITIES FOR ERBIUM(III) IN THREE HOST MATERIALS

	λ(nm)	τ_{meas} (μsec)	$\Sigma A(\text{s}^{-1})$	$W(\sec^{-1})$
$2ErF_3:57ZrF_4:34BaF_2:3LaF_3:4AlF_3$				
$^4S_{3/2} \rightarrow {}^4I_{15/2}$	555	290	1586	1862
$^4F_{9/2} \rightarrow {}^4I_{15/2}$	666	169	1375	4542
$^4S_{3/2} \rightarrow {}^4I_{13/2}$	853	289	1586	1862
2 wt% ErF_3 in $46PbF_2:30GaF_3:22ZnF_2:2LaF_3$				
$^4S_{3/2} \rightarrow {}^4I_{15/2}$	547	321	2361	754
$^4F_{9/2} \rightarrow {}^4I_{15/2}$	665	358	1264	1529
$^4S_{3/2} \rightarrow {}^4I_{13/2}$	846	321	2361	754
Cubic crystal $Er_{0.0038}Y_{0.498}Zr_{0.498}O_{1.748}$				
$^4S_{3/2} \rightarrow {}^4I_{15/2}$	554	141	3083	4009
$^4F_{9/2} \rightarrow {}^4I_{15/2}$	671	151	1820	4803
$^4S_{3/2} \rightarrow {}^4I_{13/2}$	853	145	3083	4009

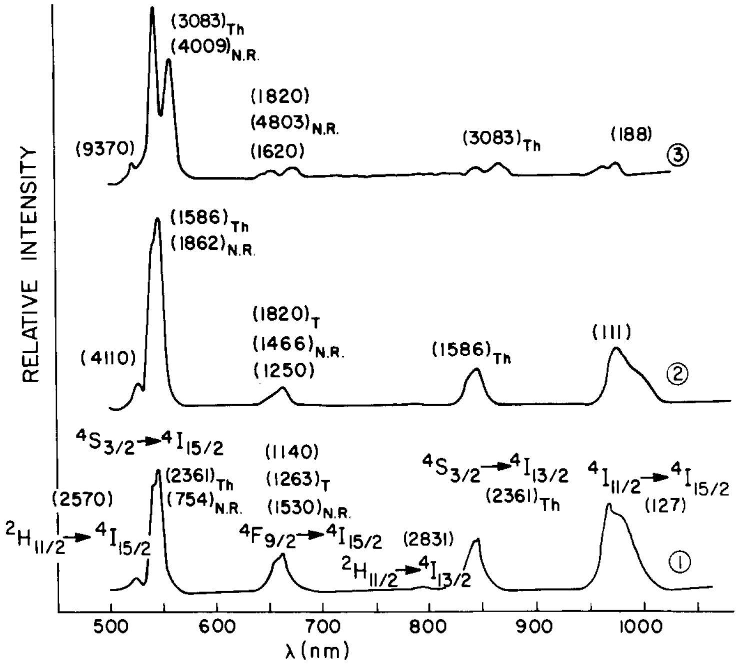

FIG. 3. Comparison of emission spectra of erbium(III) in two fluoride glasses and in the crystalline mixed zirconium–yttrium oxide, at 300 K. The transition probabilities (in sec^{-1}) given in parentheses are defined in the text. (1) 2.00 wt% $ErF_3 \cdot 46PbF_2 \cdot 22ZnF_2 \cdot 30GaF_3 \cdot 2LaF_3$ (mole%) glass. (2) 2.66 wt% $ErF_3 \cdot 57ZrF_4 \cdot 34BaF_2 \cdot 3LaF_3 \cdot 4AlF_3$ (mole%) glass. (3) 0.55 wt% $Er_2O_3 \cdot 67ZrO_2 \cdot 33Y_2O_3$ (mole%) stabilized cubic crystal. λ_{excit} = 490 nm, $^4F_{7/2}$; PMT S-1 detector.

TABLE V

SELECTED POSSIBLE LASER TRANSITIONS OF ERBIUM(III) IN THE GLASS $57ZrF_4 : 34BaF_2 : 3LaF_3 : 4AlF_3 : 2ErF_3$

Transition	Wavelength (nm)	Radiative A(s^{-1})	Branching ratio β_{12}	Peak cross section σ_p(10^{-20} cm^2)
$^4G_{11/2} \rightarrow {}^4I_{15/2}$	378	14900	0.859	3.719
$^2H_{9/2} \rightarrow {}^4I_{15/2}$	405	1030	0.394	0.453
$^4F_{3/2} \rightarrow {}^4I_{15/2}$	440	1000	0.457	0.524
$^4F_{5/2} \rightarrow {}^4I_{15/2}$	448	1070	0.434	0.939
$^4F_{7/2} \rightarrow {}^4I_{15/2}$	486	2430	0.750	1.770
$^2H_{11/2} \rightarrow {}^4I_{15/2}$	519	4110	0.932	2.538
$^4S_{3/2} \rightarrow {}^4I_{15/2}$	540	886	0.656	0.702
$^2H_{9/2} \rightarrow {}^4I_{13/2}$	551	1150	0.442	—
$^4F_{9/2} \rightarrow {}^4I_{15/2}$	650	1250	0.909	1.119
$^2H_{11/2} \rightarrow {}^4I_{13/2}$	786	158	0.036	—
$^4I_{9/2} \rightarrow {}^4I_{15/2}$	795	148	0.774	0.192
$^4S_{3/2} \rightarrow {}^4I_{13/2}$	835	383	0.284	—
$^4I_{11/2} \rightarrow {}^4I_{15/2}$	975	111	0.820	0.372
$^2H_{11/2} \rightarrow {}^4I_{9/2}$	1495	640	0.014	—
$^4I_{13/2} \rightarrow {}^4I_{15/2}$	1529	122	1.000	0.577
$^4I_{11/2} \rightarrow {}^4I_{13/2}$	2691	24	0.180	—

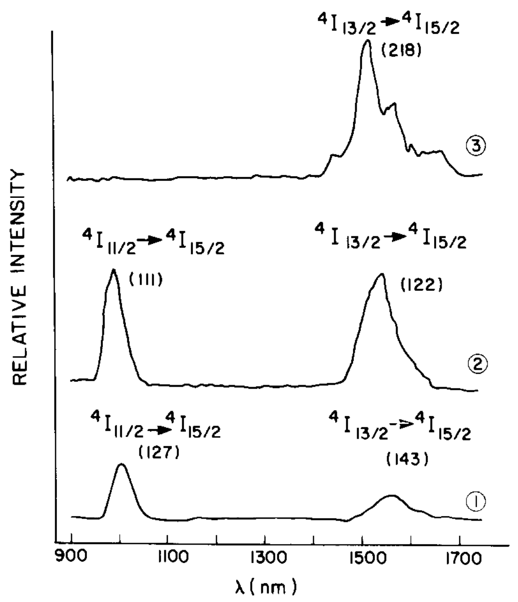

FIG. 4. Emission spectra of erbium(III) in the near infrared, at 300 K. (1) 2.00 wt% $ErF_3 \cdot 46PbF_2 \cdot 22ZnF_2 \cdot 30GaF_3 \cdot 2LaF_3$ (mole%) glass. (2) 2.66 wt% $ErF_3 \cdot 57ZrF_4 \cdot 34BaF_2 \cdot 3LaF_3 \cdot 4AlF_3$ (mole%) glass. (3) 0.55 wt% $Er_2O_3 \cdot 67ZrO_2 \cdot 33Y_2O_3$ (mole%) stabilized cubic crystal. λ_{excit} = 650 nm, $^4F_{9/2}$; PbS detector.

tions from $^4S_{3/2}$ and one from $^4F_{9/2}$) with the value of $\Sigma A(\sec^{-1})$ listed in Table III (A_{eff} in the case of the $^4S_{3/2}$ state thermalizing with the $^2H_{11/2}$) state and with $W(\sec^{-1})$ for nonradiative transitions derived from Eq. (1). Corresponding to the unusually small importance of nonradiative relaxation in the two fluoride glasses, the value of 0.3 msec of the measured lifetimes for these three transitions is exceptionally high.

In continuation of Table IV of Ref. (*8*) and of Table V of Ref. (*9*), Table V gives selected possible laser transitions for Er(III) in the zirconium–barium fluoride glass. The peak cross section for stimulated emission $\sigma_p = \lambda^4 A/(8\pi c^2 n \Delta\lambda)$ is given in units of 10^{-20} cm^2 where n is the refractive index and $\Delta\lambda$ the effective fluorescence line width (*12*). Whereas the four-level laser situations with $^4I_{13/2}$ (or higher states) as terminal levels have rather low branching ratios (the $^2H_{9/2}$ state providing the most favorable branching ratio at 551 nm is likely to have strong problems of nonradiative competition because of the modest energy gap 2000 cm^{-1} to the $^4F_{3/2}$ level in Table I), the other transitions in Table V correspond formally to three-level lasers. However, the sublevel spreading of $^4I_{15/2}$ in each erbium site in the glass is likely to be a few hundred cm^{-1} and four-level operation is still conceivable at low erbium concentrations and perhaps by cooling with liquid air. This question is partly decided by the question of energy transfer between differing Er(III) in the glass (*27*).

4. Conclusions

Er(III), in both the lead–gallium–zinc fluoride glass discussed in the previous paper (*8*) and in the zirconium–barium fluoride glass studied here, shows a remarkable propensity of narrow-band luminescence from several excited J levels, as seen from Table IV and Fig. 3. Strong emission is observed from the first, second, fourth, and fifth excited levels in Table I, that is, as soon as the energy gap is at least 2800 cm^{-1}. This can be explained mainly by the low phonon energy in fluoride glasses, and is also known (*18*) to permit exceptionally strong emission from $^5D_1$, $^5D_2$, and $^5D_3$ in Eu(III). The main difference between the two kinds of fluoride glasses treated here is that Ω_2 (and hence the hypersensitive pseudo-quadrupolar transitions) is about twice as strong in the glass containing zirconium and barium. Nevertheless, the branching ratios in Table III are not dramatically different for the transitions likely to show a high yield of luminescence.

Since the undoped materials are excellent candidates for fiber optic waveguides due to their high transmittance in the infrared and their chemical stability, it is suggested that the erbium doped materials having the desired laser emission wavelengths, which can be selected from Table V, be used as light sources for fiber optic systems. They could be integrated into one waveguide providing integrated fiber optic systems.

References

1. M. Poulain, M. Poulain, and J. Lucas, *Mater. Res. Bull.* **10,** 243 (1975).
2. M. Poulain, M. Chanthanasinh, and J. Lucas, *Mater. Res. Bull.* **12,** 151 (1977).
3. M. Poulain and J. Lucas, *Verres Refract.* **32,** 505 (1978).
4. M. G. Drexhage, C. T. Moynihan, M. Saleh Boulos, and K. P. Quinlan, Proc. Conf. Phys. Fiber Optics (B. Bendow and S. S. Mitra, Eds.), Amer. Ceramic Soc., Columbus, Ohio (1981).
5. B. Bendow, R. N. Brown, M. G. Drexhage, T. J. Loretz, and R. L. Kirk, *Appl. Opt.* **20,** 3688 (1981).
6. B. Bendow, M. G. Drexhage, and H. G. Lipson, *J. Appl. Phys.* **52,** 1460 (1981).
7. J. Lucas, M. Chanthanasinh, M. Poulain, M. Poulain, P. Brun, and M. J. Weber, *J. Non-Crystalline Solids* **27,** 273 (1978).
8. R. Reisfeld, G. Katz, N. Spector, C. K. Jørgensen, C. Jacoboni, and R. DePape, *J. Solid State Chem.* **41,** 253 (1982).
9. E. Greenberg, G. Katz, R. Reisfeld, N. Spector, R. C. Marshall, B. Bendow, and R. N. Brown, *J. Chem. Phys.* **77,** 4797 (1982).
10. C. K. Jørgensen and R. Reisfeld, *Top. Curr. Chem.* **100,** 127 (1982).
11. R. D. Peacock, *Struct. Bonding* **22,** 83 (1975).
12. R. Reisfeld and C. K. Jørgensen, "Lasers and Excited States of Rare Earths," Springer-Verlag, Berlin (1977).
13. W. T. Carnall, P. R. Fields, and K. Rajnak, *J. Chem. Phys.* **49,** 4412, 4424, 4443, 4447, and 4450 (1968).
14. R. Reisfeld and Y. Eckstein, *J. Chem. Phys.* **63,** 4001 (1975).
15. R. Reisfeld and J. Hormadaly, *J. Chem. Phys.* **64,** 3207 (1976).
16. R. Reisfeld, *Struct. Bonding* **22,** 123 (1975).
17. B. Blanzat, L. Boehm, C. K. Jørgensen, R. Reisfeld, and N. Spector, *J. Solid State Chem.* **32,** 195 (1980).
18. R. Reisfeld, E. Greenberg, R. N. Brown, M. G. Drexhage, and C. K. Jørgensen, *Chem. Phys. Lett.* **95,** 91 (1983).
19. M. Robinson, R. C. Pastor, R. R. Turk, D. P. Devor, and M. Braunstein, *Mater. Res. Bull.* **15,** 735 (1980).
20. Y. Kalisky, R. Reisfeld, and Y. Haas, *Chem. Phys. Lett.* **61,** 19 (1979).
21. W. F. Krupke, *Phys. Rev.* **145,** 325 (1966).
22. G. N. Papatheodorou and R. W. Berg, *Chem. Phys. Lett.* **75,** 483 (1980).
23. B. R. Judd, *J. Chem. Phys.* **70,** 4830 (1979).
24. C. K. Jørgensen, *Top. Curr. Chem.* **56,** 1 (1975).
25. C. K. Jørgensen, "Physics and Chemistry of Rare Earths" (K. Gschneidner and L. Eyring, Eds.), Vol. 3, p. 111, North–Holland, Amsterdam (1979).
26. G. Boulon, C. K. Jørgensen, and R. Reisfeld, *Chem. Phys. Lett.* **75,** 24 (1980).
27. R. Reisfeld, E. Greenberg, C. Jacoboni, R. DePape, and C. K. Jørgensen, *J. Solid State Chem.*, to be submitted.
28. W. T. Carnall, J. P. Hessler, and F. Wagner, *J. Phys. Chem.* **82,** 2152 (1978).
29. J. P. Miranday, C. Jacoboni, and R. DePape, *J. Non-Crystalline Solids* **43,** 393 (1981).
30. J. P. Miranday, C. Jacoboni, and R. DePape, *Rev. Chim. Minér.* **16,** 277 (1979).